Development 136, 1509-1517 (2009) doi:10.1242/dev.025932

A gain-of-function mutation in *IAA18* alters *Arabidopsis* embryonic apical patterning

Sara E. Ploense, Miin-Feng Wu, Punita Nagpal and Jason W. Reed*

Lateral organ emergence in plant embryos and meristems depends on spatially coordinated auxin transport and auxin response. Here, we report the gain-of-function *iaa18-1* mutation in *Arabidopsis*, which stabilizes the Aux/IAA protein IAA18 and causes aberrant cotyledon placement in embryos. *IAA18* was expressed in the apical domain of globular stage embryos, and in the shoot apical meristem and adaxial domain of cotyledons of heart stage embryos. Mutant globular embryos had asymmetric PIN1:GFP expression in the apical domain, indicating that IAA18-1 disrupts auxin transport. Genetic interactions among *iaa18-1*, loss-of-function mutations in *ARF* (Auxin response factor) genes and *ARF*-overexpressing constructs suggest that IAA18-1 inhibits activity of MP/ARF5 and other ARF proteins in the apical domain. The *iaa18-1* mutation also increased the frequency of rootless seedlings in mutant backgrounds in which auxin regulation of basal pole development was affected. These results indicate that apical patterning requires Aux/IAA protein turnover, and that apical domain auxin response also influences root formation.

KEY WORDS: Auxin, Aux/IAA, Phyllotaxy, Embryo

INTRODUCTION

Plant embryos provide a simple context in which to study patterning and differentiation events that are reiterated at later stages. In *Arabidopsis*, cotyledon placement and outgrowth, flower meristem formation, and flower organ emergence all require the auxin-responsive transcription factor MP/ARF5 and the auxin efflux transporter PIN1, indicating that apical patterning in embryos and adults share mechanisms (Berleth and Jürgens, 1993; Hardtke et al., 2004; Okada et al., 1991; Przemeck et al., 1996). Thus, studies of cotyledon formation in embryos may reveal how patterning occurs de novo and provide insight into how organs form postembryonically.

Auxin regulates gene expression by inducing turnover of Aux/IAA proteins. Aux/IAA proteins dimerize with Auxin response factor (ARF) transcription factors through shared C-terminal motifs, and inhibit gene induction through a conserved sequence in Aux/IAA proteins called motif I (Szemenyei et al., 2008; Tiwari et al., 2004; Tiwari et al., 2001). In the presence of auxin, F-box auxin receptors TIR1 and AFB1-AFB3 (and possibly also AFB4 and AFB5) bind to a conserved sequence called motif II in Aux/IAA proteins, leading to Aux/IAA protein ubiquitination by SCF complexes and subsequent turnover by the proteasome (Dharmasiri et al., 2005a; Dharmasiri et al., 2003; Dharmasiri et al., 2005b; Gray et al., 2001; Kepinski and Leyser, 2004; Kepinski and Leyser, 2005; Ramos et al., 2001; Tan et al., 2007; Tian et al., 2003; Walsh et al., 2006; Zenser et al., 2001). Auxin-induced Aux/IAA turnover frees ARF proteins to activate target genes (Guilfoyle and Hagen, 2007; Ulmasov et al., 1997a; Ulmasov et al., 1999a; Ulmasov et al., 1999b). Dominant or semi-dominant missense mutations that affect motif II in *Arabidopsis IAA* genes decrease interaction of the corresponding Aux/IAA proteins with auxin receptors and thereby stabilize them (Dharmasiri et al., 2005b; Gray et al., 2001; Kepinski and Leyser, 2004; Kepinski and Leyser, 2005; Reed, 2001; Tatematsu et al., 2004; Tian et al., 2003; Yang et al., 2004). In most cases, gain-of-function *iaa* mutations decrease auxin response, consistent with the model that Aux/IAA proteins inhibit gene activation by ARFs. However, gain-of-function *axr3* mutations in *AXR3/IAA17* increase response to auxin in some assays (Leyser et al., 1996).

Both root formation and shoot patterning in *Arabidopsis* embryos require auxin-regulated gene expression responses. *mp* (*monopteros*) mutants deficient in MP/ARF5, gain-of-function mutations in *BODENLOS*(*BDL*)*/IAA12* or *IAA13*, and embryos lacking multiple auxin receptors lack the hypophysis (the precursor of the root cap and quiescent center) and fail to form a primary root (Berleth and Jürgens, 1993; Dharmasiri et al., 2005b; Hamann et al., 2002; Hamann et al., 1999; Weijers et al., 2005a). Hypophysis formation requires MP/ARF5 activity in overlying pro-embryo axis cells (Weijers et al., 2006). These studies have led to the model that BDL/IAA12 and IAA13 regulate MP/ARF5 activity in the axis. *axr3* embryos form a root but have aberrant root cap cell morphology, indicating that auxin also regulates embryonic root cell differentiation (Sabatini et al., 1999).

In the embryonic shoot, *mp* mutations cause frequent cotyledon fusions and vascular patterning defects (Aida et al., 2002; Berleth and Jürgens, 1993; Hardtke and Berleth, 1998; Przemeck et al., 1996). *nph4* (*non-phototropic hypocotyl*) single mutants defective in *NPH4/ARF7* have normal embryo patterning, but *mp nph4* double mutants lack both root and shoot organs (Hardtke et al., 2004). Mutation of the *miR160* target site in *ARF17*, which may cause increased or ectopic expression of *ARF17*, causes defects in leaf shape, cotyledon outgrowth and flower morphology (Mallory et al., 2005). *tir1 afb2 afb3* triple and *tir1 afb1 afb2 afb3* quadruple auxin receptor mutants also often have aberrant cotyledon outgrowth (Dharmasiri et al., 2005b), although Aux/IAA proteins that act in the apical domain to regulate patterning have not been identified.

Auxin movement also contributes to correct patterning. PIN1 and other related proteins are required for auxin efflux, and their polar localization in plasma membranes have suggested routes of auxin movement in embryos, meristems and other tissues (Benkova et al., 2003; Friml et al., 2002; Friml et al., 2003; Galweiler et al., 1998; Heisler et al., 2005; Reinhardt et al., 2000; Reinhardt et al., 2003).

Department of Biology, University of North Carolina at Chapel Hill, Coker Hall, Chapel Hill, NC 27599, USA.

*Author for correspondence (e-mail: jreed@email.unc.edu)

Accepted 27 February 2009

pin1 mutants frequently have fused cotyledons, fail to form flowers on inflorescence meristems, and have fewer organs in rare flowers that do form (Aida et al., 2002; Furutani et al., 2004; Okada et al., 1991; Vernoux et al., 2000). PIN2, PIN3, PIN4 and PIN7 also contribute to embryo patterning, and *pinoid* mutants with defects in PIN localization also have phyllotactic defects (Benjamins et al., 2001; Bennett et al., 1995; Blilou et al., 2005; Friml et al., 2002; Friml et al., 2004; Vieten et al., 2005; Weijers et al., 2005b). *PIN* genes and PIN proteins are subject to positive and negative feedback. Auxin regulates *PIN* and *PID* genes, and individual *pin* mutations cause other *PIN* genes to be expressed in expanded domains (Benjamins et al., 2001; Blilou et al., 2005; Vieten et al., 2005). Auxin also inhibits PIN protein endocytosis and it can affect PIN polar localization (Paciorek et al., 2005; Sauer et al., 2006a). *mp pin1* mutants and *mp* mutants treated with an auxin transport inhibitor have no leaves, indicating that auxin transport and MP/ARF5 have partly independent effects in shoot apical meristems (Schuetz et al., 2008).

Here, we describe the *iaa18-1* gain-of-function mutation in *IAA18*, which stabilizes an Aux/IAA protein that is expressed in the apical domain of embryos. The mutation affects PIN1 expression in the apical domain, and causes aberrant cotyledon positioning and outgrowth.

MATERIALS AND METHODS

Plant material

The *iaa18-1* mutant was backcrossed six times to the Landsberg *erecta* (L*er*) ecotype prior to detailed characterization. *mp-CSH1* and *bdl-1* mutations are in the L*er* ecotype, and *axr1-13*, *axr6-1* and *nph4-1* mutations are in Columbia (Col) ecotype (Hamann et al., 1999; Hardtke and Berleth, 1998; Hobbie et al., 2000; Liscum and Briggs, 1996) (M.-R. Cha and M. Estelle, personal communication). Plants were genotyped by PCR using CAPS, dCAPS or T-DNA border markers. *PIN1:GFP* fusion plants in both L*er* (Heisler et al., 2005) and Col (Benkova et al., 2003) backgrounds were used.

Plasmid construction and generation of transgenic plants

N-terminal and full-length *IAA18* genomic fragments were amplified from wild-type or *iaa18-1* plants by PCR using a 5′ primer covering the *Pst*I site 2576 bp upstream of the *IAA18* start codon and 3′ primers terminating at either C135 or R267 of the coding sequence or 334 bp downstream of the stop codon. Genomic fragments were subcloned, sequenced and subsequently inserted into the *Pst*I and *Bam*HI sites of the pCAMBIA 1391Xa vector (CAMBIA, Canberra, Australia) to generate translational *IAA18:GUS* fusions, or into the pPZP211 vector (Hajdukiewicz et al., 1994) to generate the *iaa18-1* plasmid. Introduction of a *Bam*HI site into the 3′ primers generated a C135W mutation in the *IAA18NT:GUS* and *iaa18-1NT:GUS* plasmids, and an additional R at the C terminus of the *IAA18:GUS* and *iaa18-1:GUS* plasmids. Constructs were introduced into wild-type L*er* plants by the floral dip method. T1 transformed seedlings were selected on plates containing hygromycin, transferred to soil and allowed to self-fertilize. For *IAA18NT:GUS*, *iaa18-1NT:GUS* and *IAA18:GUS* constructs, GUS activity was assayed among progeny of at least 16 primary transformants. Transformed lines carrying the same construct exhibited qualitatively similar staining patterns with some variation in intensity. Transformants with single loci of the constructs were selected for subsequent analyses and crossing into mutant backgrounds. Reporter gene activities in Col/L*er* mixed backgrounds were consistent among F3 and F4 progeny of at least three independent F2 lines. *iaa18-1* or *iaa18-1:GUS* constructs were silenced in all surviving T1 plants and their progeny.

For P_{35S}*:ARF6* and P_{35S}*:ARF8* constructs, *ARF6* or *ARF8* cDNA sequences were amplified with primers flanking the coding region, cloned into pENTR/D-TOPO (Invitrogen) and subcloned into pB2GW7 using LR clonase (Karimi et al., 2002). Primers used for RT-PCR were: *MP/ARF5*, 5′-GGAGATGATCCATGGGAAGAGT-3′ and 5′-GTTAATGCCTGCGCTGTTCA-3′; *ARF6*, 5′-CACCTTTGTGAAGGTGTACAAGTC-3′ and 5′-ACGTCGTTCTCTCGGTCAAC-3′; *NPH4/ARF7*, 5′-GCGATGATCCATGGGAAGA-3′ and 5′-GCGATGATCCATGGGAAGA-3′; *ARF8*, 5′-CACGAGCTGCGAGAAGAGTTAG-3′ and 5′-CAAACGTTATTCACAAATGACTCC-3′; and *UBQ10*, 5′-AACTATCACTTTGGAGGTGGAGA-3′ and 5′-TGTGGACTCCTTCTGAATGTTG-3′.

For the *UAS:iaa18-1* construct, a *Hin*dIII-*Bam*HI fragment with the *GAL4 UAS* from pSDM7023 (Weijers et al., 2005b) was subcloned into pB7WG2 (Karimi et al., 2002) to obtain pB7WG2-UAS, in which the *UAS* fragment replaced the P_{35S} promoter. *iaa18-1* cDNA was reverse transcribed from 10-day-old seedlings and PCR amplified using primers 5′-CACCACTAGTATGGAGGGTTATTCAAGAAA-3′ and 5′-CCGAGCTCTCATCTTCTCATTTTCTCTT-3′. The PCR product was cloned into pENTR/D-TOPO and subcloned into pB7WG2-UAS using LR clonase (Invitrogen).

Histology and microscopy

For β-glucuronidase staining, seedlings and ovules were fixed in cold 90% acetone for 20-30 minutes, washed three to four times for 5 minutes in cold 50 mM PO_4 buffer and stained at 37°C for 1 to 16 hours in 50 mM PO_4 buffer (pH 7.2), 0.5 mM potassium ferro/ferricyanide and 1 μg/ml 5-Bromo-4-chloro-3-indolyl-β-D glucuronic acid (X-Gluc). Seedlings were cleared in a 70, 80 and 95% ethanol series, mounted in chlorohydrate:water (8:3) and photographed either with a Wild stereomicroscope or a Nikon E800 photomicroscope equipped with a SPOT cooled color digital camera using differential interference contrast (DIC) optics.

X-Gluc staining was very similar in embryos extruded from both acetone fixed and unfixed ovules. Both protocols were employed. Early stage embryos were released from dissected ovules by forcing tissue submerged in staining buffer through fine steel mesh. Late stage embryos were hand dissected from ovules. Embryos were stained at 37°C for 4 to 16 hours in watch glasses sealed in humidified chambers, mounted directly in 5% glycerol and photographed under an oil immersion 100× objective using DIC optics.

Propidium iodide-stained roots were imaged using a Leica TCS NT/SP confocal microscope with excitation at 488 nm (Truernit et al., 2006). For imaging PIN1:GFP in embryos (Fig. 4), *PIN1:GFP* (Heisler et al., 2005) gynoecia were fertilized with either wild-type or *iaa18-1* homozygous pollen and ovules were harvested 3 to 7 days later, fixed in 4% paraformaldehyde/1×PBS overnight and stained with DAPI (1 μg/ml in 1x PBS) (Sauer et al., 2006b). F1 embryos were extruded from ovules into 1×PBS, 5% glycerol, 0.01% Tween-20) and mounted on slides. Stacks of 1 μm optical sections were acquired on a Zeiss 510 LSM Meta confocal microscope using an oil immersion 40× objective. To image GFP and DAPI together, we used multitracking in line-scan mode. For GFP we used a 488 nm laser line attenuated to 10% and a 505-530 nm band pass filter. For DAPI we used a 364 laser line attenuated to 5% and a 385-470 nm band pass filter. Wild-type and *iaa18-1/+* embryos were photographed under identical settings. Images in Fig. S3 in the supplementary material were taken on a Zeiss DUO confocal microscope.

In situ hybridization

An *IAA18* fragment was amplified from first-strand cDNA as described above, and was cloned into pGEM-T vector (Promega). The plasmid was linearized by *Spe*I digestion and the antisense probe was synthesized by in vitro transcription with SP6 RNA polymerase using a DIG RNA labeling kit (Roche). In situ hybridization was performed as described previously (Long and Barton, 1998).

RESULTS

A semi-dominant mutation in *IAA18* affects cotyledon outgrowth

Among progeny of EMS-mutagenized Landsberg *erecta* seed, we found the *iaa18-1* mutant as a dwarfed plant with leaves that curled up (Fig. 1A-C). Homozygous mutant plants were much smaller than heterozygous plants (Fig. 1A), and segregation ratios among progeny of the mutant indicated that a single semi-dominant mutation caused both leaf curling and dwarfism (data not shown). We mapped the mutation to an interval including *IAA18*

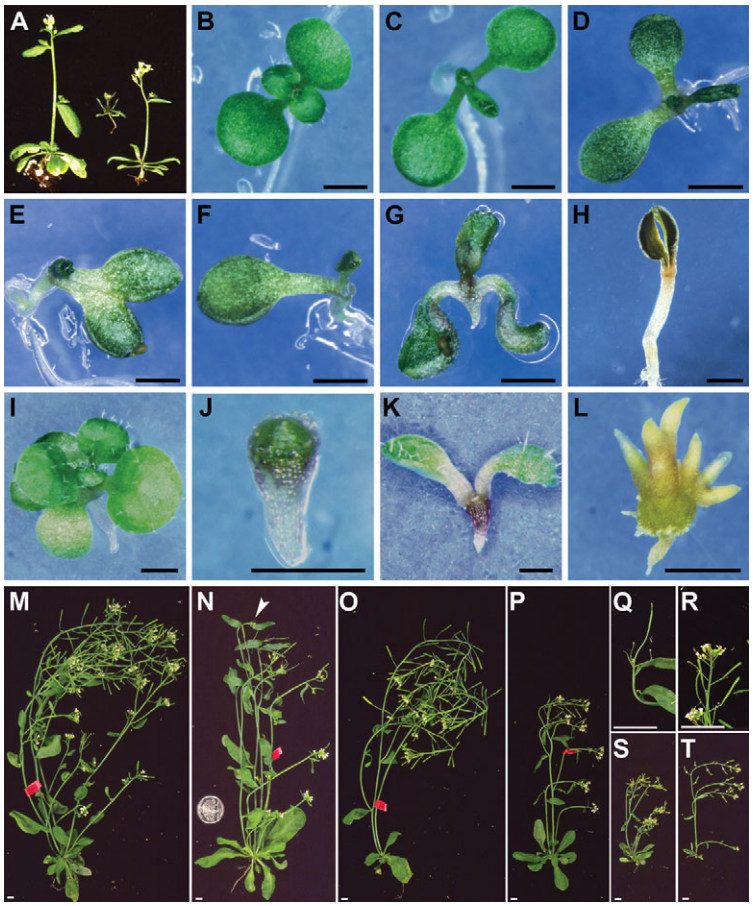

Fig. 1. Morphology of *iaa18-1* seedlings and *iaa18-1/IAA18 P$_{35S}$:MP/ARF5* plants. (**A**) Wild-type Landsberg *erecta* (L*er*, left), homozygous *iaa18-1* (center) and *iaa18-1/IAA18* (right) adult plants. (**B**) Seven-day-old L*er* seedling. (C-H) Seven-day-old *iaa18-1/* seedlings of different phenotypic classes. (**C**) *iaa18-1/IAA18* dicot. (**D**) Asymmetric dicot. (**E**) Fused cotyledons. (**F**) Monocot. (**G**) Rootless. (**H**) Unopened cotyledons. (**I**) Twelve-day-old *mp-CSH1* seedling. (**J**) Twelve-day-old *mp-CSH1 iaa18-1* seedling. (**K**) Twelve-day-old *mp-CSH1 iaa18-1/IAA18* seedling. (**L**) Four-week-old *mp-CSH1 iaa18-1* plant. Scale bars: 1.8 mm. (**M-P**,**S**,**T**) Whole shoots of adult plants. (M) *P$_{35S}$:MP/ARF5* plant with wild-type appearance. (N) *P$_{35S}$:MP/ARF5* plant with apical terminal flowers (arrowhead). (O,P,S) *iaa18-1/IAA18 P$_{35S}$:MP/ARF5* plants lacking curled leaves and with a range of heights. (T) *iaa18-1/IAA18* plant with curled leaves. (**Q**,**R**) Inflorescence termini of *P$_{35S}$:MP/ARF5* (Q) and *iaa18-1/IAA18 P$_{35S}$:MP/ARF5* (R) plants. Scale bars: 2.5 mm. The pin-formed inflorescence and terminal flower phenotypes conferred by *P$_{35S}$:MP/ARF5* in the Landsberg *erecta* background were generally weaker than those described in the Columbia ecotype (Hardtke et al., 2004).

(At1g51950), and found a guanine to adenine transition in *IAA18* that changes the glycine codon at amino acid position 99 to glutamate in the mutant. Glycine 99 is a highly conserved residue in motif II, VGWPPV, and is important for instability of Aux/IAA proteins (Ramos et al., 2001). The *shy2-3* mutation changes the corresponding glycine of *SHY2/IAA3* to glutamate, and also causes significant phenotypes including upward leaf curling (Tian and Reed, 1999). Recently, Uehara et al. independently isolated *iaa18* mutations in the Columbia ecotype that affect the same codon as *iaa18-1* and cause very similar phenotypes (Uehara et al., 2008).

As homozygous *iaa18-1* plants were almost sterile (see below), for phenotypic analyses we used progeny of self-pollinated heterozygous plants. Three to 8% of *iaa18-1/IAA18* progeny had aberrant cotyledon outgrowth, with higher frequency in a Landsberg *erecta* (L*er*) background than in a mixed L*er*/Columbia background (Fig. 1, Table 1). Some seedlings had a single cotyledon that wrapped around the meristem to encompass more than half of the circumference of the seedling apex, or had a single cotyledon of normal appearance (monocots, Fig. 1F). Enlarged cotyledons in monocots had more veins than did cotyledons of wild-type seedlings, suggesting that they might have arisen from incomplete separation of two cotyledon primordia (data not shown). Other seedlings had two distinguishable cotyledons that were fused along one edge (fused dicots, Fig. 1E), had two cotyledons with asymmetric placement (asymmetric dicots, Fig. 1D), or had three cotyledons (tricots, not shown). These aberrant cotyledon outgrowth phenotypes occurred at higher frequency among *iaa18-1* homozygotes than among heterozygotes (data not shown). Mutant seedlings that had two cotyledons in normal locations unfolded their cotyledons more slowly than did wild-type seedlings (Fig. 1H). All seedlings with aberrant cotyledon placement or folded cotyledons later developed curled leaves, suggesting that the *iaa18-1* mutation affected cotyledon outgrowth with incomplete penetrance.

In addition to cotyledon patterning defects, mutant seedlings also had long hypocotyls when grown in the light, reduced primary root growth, differentiated cells closer to the root meristem than normal, and fewer lateral roots than wild-type seedlings (see Fig. S1 and Table S1 in the supplementary material) (Uehara et al., 2008). Mutant seedlings were visibly purple, similar to stressed wild-type seedlings. Auxin inhibited mutant root growth to a similar degree as in wild-type seedlings (see Fig. S1 in the supplementary material). A small proportion (0.1-0.3%) of progeny of self-fertilized *iaa18-1* heterozygotes lacked a root (Fig. 1G, Table 1). *iaa18-1* also increased the frequency of rootless seedlings in *bdl*, *axr1-13* and *tir1-1* backgrounds (Table 1). Flowers of homozygous plants had fewer petals and stamens than did flowers of wild-type plants (see Table S2 in the supplementary material), and they had short stamen filaments. Most ovules in homozygous mutant siliques aborted without forming a seed, even if pollinated with wild-type pollen.

Transgenic plants carrying either an *iaa18-1* genomic construct (*iaa18-1*) or a fusion of the *iaa18-1* promoter and full-length open reading frame to the *GUS* gene (*iaa18-1:GUS*) also had curled leaves, closed cotyledons and/or cotyledon phyllotaxy defects (see Materials and methods; Fig. S2 and Table S3 in the supplementary material), indicating that the *iaa18-1* mutation can cause the phenotypes we observed. Consistent with the semidominance of *iaa18-1*, different transformants had a range of phenotypes that were generally stronger than those of the original mutant, suggesting that

Table 1. Frequency of seedling phenotypes (%)

Parental genotype	*n*	Seedlings with root				Seedlings without root†		
		Asymmetric dicot	Tricot	Fused	Monocot	+ Cotyledons	– Cotyledons	Total
iaa18-1/IAA18	1548	0.4	0.1	1.7	5.7	0.1	0	7.9
*iaa18-1/IAA18**	2759	0.2	0.8	0.4	1.6	0.3	0	3.3
axr1/AXR1	854	0	0	0	0.1	0	0	0.1
*iaa18-1/IAA18 axr1/AXR1**	901	0.4	0	2.1	13.5	9.8	0	25.8
tir1-1/tir1-1	1059	0	0	0	0	0	0	0
*iaa18-1/IAA18 tir1/tir1**	728	0.7	1.4	0.4	1.9	2.6	0	7.0
mp-CSH1/MP	530	0	0	0	0	21.9	0	21.9
iaa18-1/IAA18 mp-CSH1/MP	1548	2.1	0.5	1.9	12.5	8.5	13.4	38.9
*mp-CSH1/MP nph4-1/NPH4**	355	0	0	0	0	20.1	9.3	29.4
bdl/BDL	484	0	0	1.2	0	14.4	0	15.6
iaa18-1/IAA18 bdl/BDL‡	209	2.9	0	1.4	5.3	21.0	0	30.6
*iaa18-1/IAA18 nph4-1/NPH4**	877	0.5	0.1	1.1	3.0	0	0	4.7

*Mixed Landsberg/Columbia background.
†Rootless seedlings were not scored for phyllotaxy defects other than absence of cotyledons.
‡For *iaa18-1/IAA18 bdl/BDL*, F1 seedlings were used, as double mutants could not be propagated.

these phenotypes are sensitive to *iaa18-1* gene dosage or expression level. Most T1 seedlings, including all of those with strong phenotypes, failed to survive to adulthood or to set seed, and a significant frequency also lacked a primary root (see Fig. S2, Table S3 in the supplementary material). *iaa18-1* and *iaa18-1:GUS* transgenes had similar effects, indicating that the IAA18-1:GUS fusion protein retains function.

The *iaa18-1* mutation increases IAA18 protein level

We also generated plants carrying *IAA18:GUS*, with a full-length wild-type gene fused to *GUS*, and plants carrying *IAA18NT:GUS* or *iaa18-1NT:GUS* constructs with the N-terminal region of IAA18, including motifs I and II but lacking the C-terminal dimerization domain (Fig. 2A). These plants had normal morphology, in contrast to plants with the full-length mutant *iaa18-1:GUS* construct. Apparently, the truncated fusion proteins do not interact with ARF proteins. We used these plants as reporters for *IAA18* expression, and to explore the effect of the *iaa18-1* mutation on IAA18 protein.

Plants carrying *IAA18NT:GUS* or *IAA18:GUS* constructs had X-Gluc staining in the stele of roots and vascular tissues of hypocotyl, cotyledons and leaves (Fig. 2D,E, data not shown). The staining in the root was strongest in the stele in the elongation zone just above the meristem, weaker in the meristem and in older parts of the root, and excluded from the root cap and meristem initials (Fig. 2E). Adaxial domains of developing leaf primordia also had staining (Fig. 2G), which became restricted to the vasculature as the leaves expanded, similarly to the staining in cotyledons (data not shown, Fig. 2D). Staining also appeared in chalazal pole cells of mature ovules (Fig. 3A).

Plants with the *iaa18-1NT:GUS* construct had strong X-Gluc staining throughout the hypocotyl, cotyledons and leaves, rather than just in vascular tissues as for the *IAA18:GUS* and *IAA18NT:GUS* fusions (Fig. 2D). Staining in leaf primordia appeared somewhat stronger in the adaxial domain than in the abaxial domain (Fig. 2H). In roots, *iaa18-1NT:GUS* plants had staining in the stele just behind the root meristem (Fig. 2F) and also in older parts of the root (Fig. 2D). In ovules, staining was present in cells at the chalazal pole, in the endothelium and integuments that later form the seed coat, and, to a lesser extent, in the endosperm (Fig. 3B). The *IAA18*, *iaa18-1* and fusion protein transcripts were present at comparable levels (Fig. 2C), and were not induced by auxin (Fig. 2B) (Okushima et al., 2005; Tian et al., 2002). These results indicate that the *iaa18-1* mutation increased the amount of fusion protein in mature root stele and in shoot organs, most probably by stabilizing the IAA18 protein as motif II mutations in other *IAA* genes do. IAA18-1NT:GUS protein may be present in domains where IAA18:GUS protein is absent because the wild-type reporter protein is turned over quickly in most tissues.

IAA18-1 is present in the apical domain of embryos

To ascertain in which cells IAA18-1 acts to affect cotyledon formation, we assessed *IAA18* expression pattern in embryos. In *iaa18-1NT:GUS* embryos, X-gluc staining appeared initially in the apical domain sometimes at the 16-cell stage, and with complete penetrance at the 32-cell stage (Fig. 3G). At late globular stage, staining became restricted to a strip of cells encompassing the nascent shoot apical meristem and extending through the periphery of the embryonic apex (Fig. 3H,I,A′). This apical expression pattern persisted through subsequent stages so that it became apparent that staining on the apical periphery had been restricted to cells between the cotyledons. Staining appeared on the adaxial sides of the cotyledons by mid-heart stage and this persisted through heart and early torpedo stages (Fig. 3J,K). At late torpedo and walking stick stages, staining appeared throughout the cotyledons, especially in developing vasculature, and in axis vasculature (Fig. 3L,M). Expression patterns from globular to heart stages seen by in situ hybridization with an *IAA18* antisense probe mirrored these *iaa18-1NT:GUS* staining results almost exactly (Fig. 3N-R; J. Long, personal communication), revealing that the *iaa18-1NT:GUS* reporter expression reflects the *IAA18* transcript pattern. This expression pattern, and the ability of the *iaa18-1:GUS* transgene to recapitulate all *iaa18-1* embryo phenotypes, suggest that the stabilized IAA18-1 protein acts in apical cells in globular embryos, and in adaxial and nascent shoot apical meristem domains of heart stage embryos.

In *mp-CSH1*, *iaa18-1*, *axr6-1* and *axr1-13* embryos, *iaa18-1NT:GUS* staining was present in the same apical domain as in wild-type embryos (Fig. 3U-Y). In *mp-CSH1 nph4-1* double mutant embryos, which do not form cotyledons, staining was present in the presumptive shoot apical meristem but not on the flanks (Fig. 3Z,B′). Together with the absence of auxin regulation of *IAA18* transcript level (Fig. 2B), these results suggest that ARF proteins do not regulate *IAA18* expression directly.

In contrast to *iaa18-1NT:GUS* embryos, *IAA18:GUS* and *IAA18NT:GUS* embryos expressing wild-type fusions lacked X-Gluc staining (Fig. 3A, data not shown). Some *axr1-13* and *axr6-1* mutant embryos with defects in SCF ubiquitin ligase function had

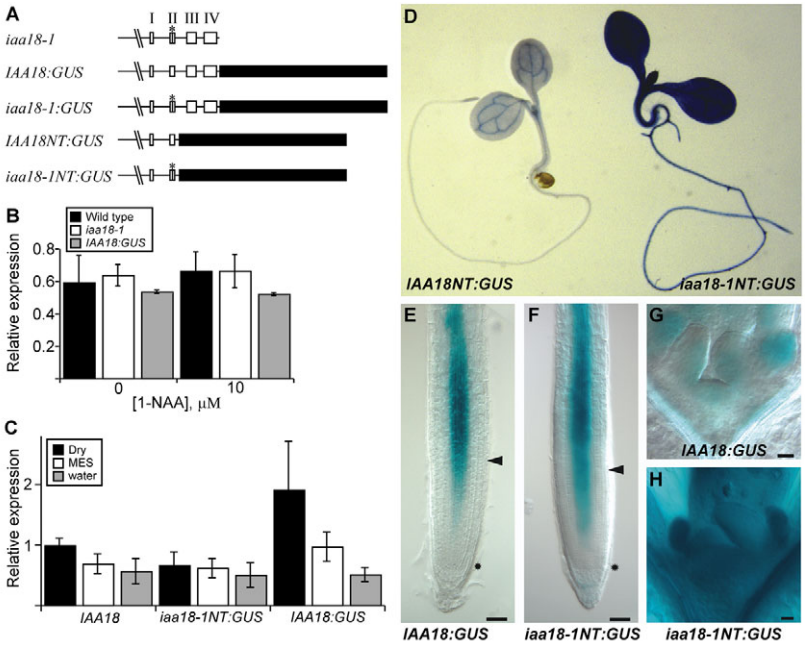

Fig. 2. Expression of *IAA18:GUS* fusion constructs in transgenic plants. (**A**) IAA18:GUS fusion constructs. White boxes, *IAA18* exons; black boxes, *GUS* gene; *, *iaa18-1* mutation. (**B**) Expression level of *IAA18* in wild-type, *iaa18-1* and *IAA18:GUS* seedlings after mock treatment or after 40 minutes of treatment with 10 μM 1-NAA. (**C**) Expression levels of *IAA18*, *iaa18NT:GUS* and *IAA18:GUS* genes either untreated (dry) or after immersion in water (pH 7.4) or 50 mM MES (pH 5.4). In B and C, signals from RNA blot hybridizations of the indicated genes were digitized and normalized to signals from β-tubulin, and then each value was normalized to the untreated wild-type value from the first experiment. Error bars indicate s.d. of normalized measurements from four (*IAA18* and *iaa18-1*) or two (*IAA18:GUS*) blots. (**D-H**) Six-day-old seedlings stained with X-gluc. (D) *IAA18NT:GUS* (left) and *iaa18-1NT:GUS* (right). (E,G) *IAA18:GUS* in root (E) and shoot (G) meristems. (F,H) *iaa18-1NT:GUS* in root (F) and shoot (H) meristems. In E and F, asterisks mark the level of the quiescent center and arrowheads indicate the point at which cells begin to elongate. Scale bars: 190 μm.

IAA18:GUS staining in the apical domain of embryos (Fig. 3S,T). SCF complexes may normally mediate efficient IAA18 turnover in the apical domain of embryos, so that the wild-type IAA18:GUS and IAA18NT:GUS fusion proteins do not accumulate to detectable levels.

iaa18-1 affects apical embryo patterning starting at globular stage

In siliques of self-pollinated *iaa18-1/IAA18* heterozygous plants, we observed heart-stage embryos with extra cells between margins of adjacent cotyledon primordia, as well as monocot embryos (Fig. 3C-F, Fig. 4K). To detect patterning phenotypes before cotyledon outgrowth, we used embryos heterozygous for *iaa18-1* and carrying a *PIN1:GFP* protein fusion construct (Heisler et al., 2005). In wild-type early globular stage embryos, PIN1:GFP was expressed throughout the apical half and in nascent provascular cells (Fig. 4A). At mid- and late-globular and transition stages, expression was highest at two foci on the flanks of the apex, and was also present in the cell tier beneath the apical half of the pro-embryo and in the provascular cells of the incipient hypocotyl (Fig. 4D,G). In heart stage embryos, expression persisted in the L1 cells of the nascent shoot apical meristem; in tips, abaxial L1 and distal adaxial L1 cells of cotyledons; and in provascular cells of the cotyledons and axis (Fig. 4J). As heart stage embryos elaborated L2 and L3 layers of the nascent shoot apical meristem, expression was lost in these cell layers.

PIN1:GFP expression in *iaa18-1/IAA18* embryos deviated from the wild-type expression pattern starting at early globular stage. Whereas in wild-type embryos expression was uniform throughout the apical half, in *iaa18-1* embryos expression was often asymmetric with stronger fluorescence on one side than the other (Fig. 4B,C,E,F,H,I). We observed such asymmetric expression in about 19% of early globular stage embryos examined, and about 40% of mid- to late-globular and transition stage embryos (see Table S4 in the supplementary material). (The overall frequency of asymmetric PIN1:GFP in wild-type embryos was about 1%.) Some *iaa18-1* transition stage embryos also had discontinuities in PIN1:GFP fluorescence in the nascent vasculature (Fig. 4H).

In addition to asymmetries in PIN1:GFP expression, *iaa18-1* globular embryos occasionally had aberrant or ectopic cell divisions in the L1 layer within a focus of strong PIN1:GFP expression. In one case, periclinal divisions of adjacent apical L1 cells were not aligned with each other, leading to disordered cell layers (Fig. 4C). In another case, an ectopic periclinal cell division occurred (Fig. 4F).

iaa18-1 heart-stage embryos often lacked PIN1:GFP fluorescence in cells in a single tier just beneath the embryonic shoot apical meristem (Fig. 4K, see Fig. S3 in the supplementary material). As seen in transition stage embryos, some *iaa18-1* heart stage embryos also had discontinuities in PIN1:GFP fluorescence in developing cotyledon vasculature (see Fig. S3 in the supplementary material). Last, at heart and torpedo stages, the axis vascular column visualized by PIN1:GFP fluorescence was narrower in *iaa18-1* embryos than in wild-type embryos (Fig. 4J,K; see Fig. S3 in the supplementary material).

In contrast to the effects on PIN1:GFP, we detected no effect of *iaa18-1* on expression of the synthetic auxin-responsive reporter genes P_{DR5}*:GUS* and P_{DR5}*:GFP* (Benkova et al., 2003; Ulmasov et al., 1997b) at globular or transition stages (data not shown). At heart or torpedo stages after morphological abnormalities appeared, some mutant embryos lacked normal P_{DR5} expression in the root pole or had a broader expression domain along the margin of fused cotyledons (see Fig. S3 in the supplementary material).

IAA18-1 can inhibit MP/ARF5 activity

mp mutants often have fused cotyledons and also have decreased PIN1:GFP expression in leaf primordia (Berleth and Jürgens, 1993; Przemeck et al., 1996; Wenzel et al., 2007), suggesting that IAA18-1 might cause embryonic phenotypes by inhibiting MP/ARF5. We found that a P_{35S}*:MP/ARF5* construct (Hardtke et al., 2004) could suppress *iaa18-1* vegetative phenotypes (Fig. 1, see Table S5 in the supplementary material). About one-third of *iaa18-1/*P_{35S}*:MP/ARF5* T1 plants had flat rather than curled leaves (Fig. 1O,P,S,T). Some of these had leaves as large as those of *IAA18* P_{35S}*:MP/ARF5* plants and were nearly as tall (Fig. 1M,O). Two *iaa18-1/iaa18-1* P_{35S}*:MP/ARF5* plants had flat leaves and produced

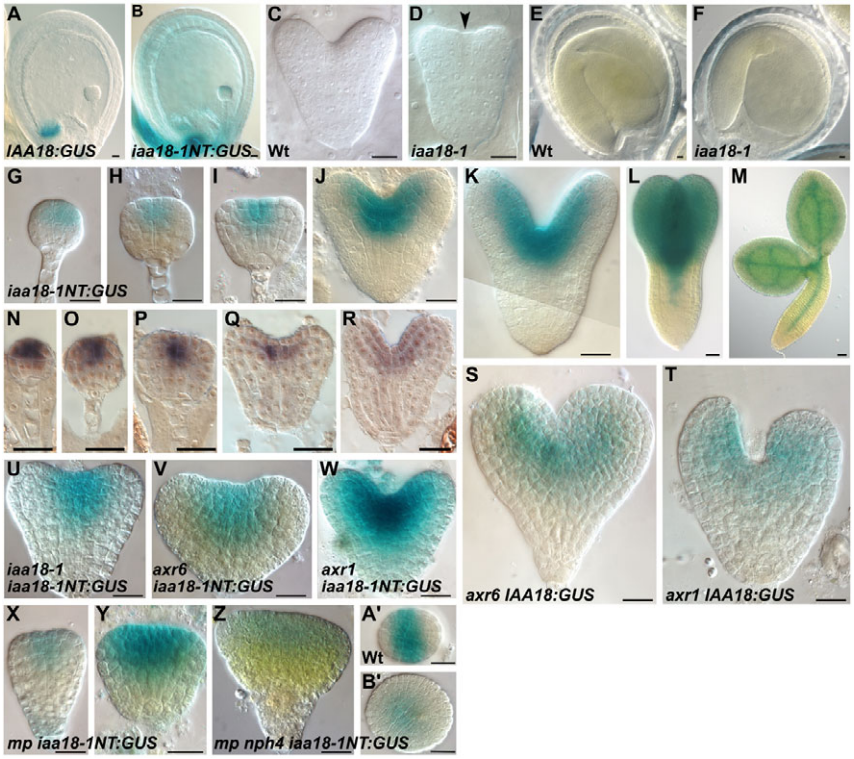

Fig. 3. Embryo phenotypes and expression of *IAA18*, *IAA18:GUS* and *iaa-18NT:GUS* in wild-type and mutant embryos. (**A**,**B**) X-gluc stained *IAA18NT:GUS* (A) and *iaa18-1NT:GUS* (B) ovules at midglobular stage. (**C**,**D**) Mid-heart stage wild-type (C) and *iaa18-1* (D) embryos. Arrowhead in D indicates overgrowth of cells at the cotyledon margin of the mutant embryo. (**E**,**F**) Mature wild-type (E) and *iaa18-1* monocot (F) embryos. (**G-M**,**A'**) X-Gluc-stained *iaa18-1NT:GUS* embryos. (**N-R**) In situ hybridization of wild-type embryos using an *IAA18* probe. (G,N) Early globular stage. (H,O) Late globular stage. (I,P,A') Transition stage. (J,Q) Mid heart stage. (K,R) Late heart stage. (L) Torpedo stage. (M) Mature embryo. (**S**) *axr6-1 IAA18:GUS* embryo. About one-quarter of F2 embryos on *axr6-1/AXR6 IAA18:GUS/-* F1 plants stained, but fewer did in subsequent generations, suggesting possible *IAA18:GUS* transgene silencing in the *axr6-1* background. (**T**) *axr1-13 IAA18:GUS* embryo. Fewer than 1% of *axr1-13 IAA18:GUS* embryos stained, perhaps because *AXR1* has an additional paralog (Dharmasiri et al., 2007). (**U**) *iaa18-1 iaa18-1NT:GUS* heart stage embryo. (**V**) *axr6-1 iaa18-1NT:GUS* heart stage embryo. (**W**) *axr1-13 iaa18-1NT:GUS* heart stage embryo. (**X**,**Y**) *mp-CSH1 iaa18-1NT:GUS* early globular and transition stage embryos. (**Z**,**B'**) *mp-CSH1 nph4-1 iaa18-1NT:GUS* heart stage embryos. A' and B' show top-down views of the embryo shoot apex. Mutant embryos were staged according to size compared with wild-type embryos. Scale bars: 10 μm. Unless indicated otherwise, X-Gluc stained embryos shown have the *iaa18-1NT:GUS* construct.

significant yields of seeds. Thus, overexpressing *MP/ARF5* could rescue leaf curling, stem elongation and fertility defects of *iaa18-1*. Conversely, the *iaa18-1* mutation appeared to suppress the *P35S:MP/ARF5* terminal flower phenotype (Fig. 1N,Q,R, see Table S5 in the supplementary material). These data indicate that IAA18-1 and MP/ARF5 can antagonize each other in plants.

To test whether IAA18-1 protein can inhibit endogenous MP/ARF5 activity in embryos, we expressed *iaa18-1* in the central domain of the embryonic axis by transforming a *UAS:iaa18-1* construct into the *GAL4:VP16*-expressing driver line *Q0990* (Haseloff et al., 1999; Weijers et al., 2006). Of 18 *Q0990 UAS:iaa18-1* T1 plants we obtained, 16 lacked a root. Of these, four had two cotyledons, five had fused cotyledons and seven were monocots (see Fig. S4 in the supplementary material). Thus, *iaa18-1* can produce a *mp*-like embryo phenotype when expressed in the domain crucial for MP/ARF5 function.

However, *iaa18-1* and *mp-CSH1* mutations enhanced each other, indicating that IAA18-1 must also affect targets other than MP/ARF5. Whereas *iaa18-1* and *mp-CSH1* single mutants always had at least one cotyledon, *mp-CSH1 iaa18-1/* seedlings (either homozygous or heterozygous for *iaa18-1*) often lacked cotyledons and sometimes also leaves (Fig. 1I,J,K; Table 1). After several weeks, some *mp-CSH1 iaa18-1/* double mutant seedlings developed radialized finger-like organs from the apex resembling those of *mp pin1* seedlings (Fig. 1L) (Schuetz et al., 2008). Occasionally, these had pistil-like tissue at the tip (data not shown).

Other candidate IAA18-1 targets closely related to MP/ARF5 include NPH4/ARF7, ARF6 and ARF8. The *nph4-1* mutation did not enhance the frequency of apical patterning defects of *iaa18-1* seedlings (Table 1), suggesting that IAA18-1 inhibits NPH4/ARF7 in embryos. However, a *P35S:NPH4/ARF7* construct (Hardtke et al., 2004), as well as *P35S:ARF6* and *P35S:ARF8* constructs, each failed to suppress *iaa18-1* vegetative phenotypes (see Table S5 in the supplementary material).

Quantitative real-time RT-PCR experiments revealed that *MP/ARF5* transcript was present at 15-75 times the wild-type level in shoots of 2-week-old T2 plants from four different *iaa18-1/P35S:MP/ARF5* lines with suppressed phenotypes (see Fig. S5 in the supplementary material). Similar analyses of four to five lines each carrying the other overexpression constructs revealed only up to sixfold increases over control transcript levels in *P35S:ARF6* or *P35S:ARF8* lines, and up to 15-fold increases in *P35S:NPH4/ARF7* lines (see Fig. S5 in the supplementary material).

The *bdl* mutation interacted similarly to *iaa18-1* with *ARF* overexpression constructs. In particular, *P35S:MP/ARF5* suppressed the curled leaf and dwarfed stature of *bdl* mutant plants, but *P35S:NPH4*, *P35S:ARF6*, and *P35S:ARF8* did not (Hardtke et al., 2004) (Table S5 in the supplementary material). *bdl/BDL iaa18-1/IAA18* embryos retained cotyledons (Table 1), suggesting that neither BDL nor IAA18-1 (nor both together) completely inhibited ARF activity in domains relevant for cotyledon outgrowth. Plants with loss-of-function mutations in *IAA12/BDL* (SALK138684) or *IAA18* (S.E.P., J. M. Alonso, J. R. Ecker and J.W.R., unpublished), and double loss-of-function *iaa12 iaa18* mutant plants developed normally (data not shown).

DISCUSSION

IAA18-1 affects apical patterning

IAA18-1 is present throughout the apical domain of globular stage embryos, and its turnover is required for correct PIN1:GFP expression and for proper cotyledon outgrowth. As *iaa18-1* patterning defects resemble those of *pin1* and *pinoid* mutants (Aida

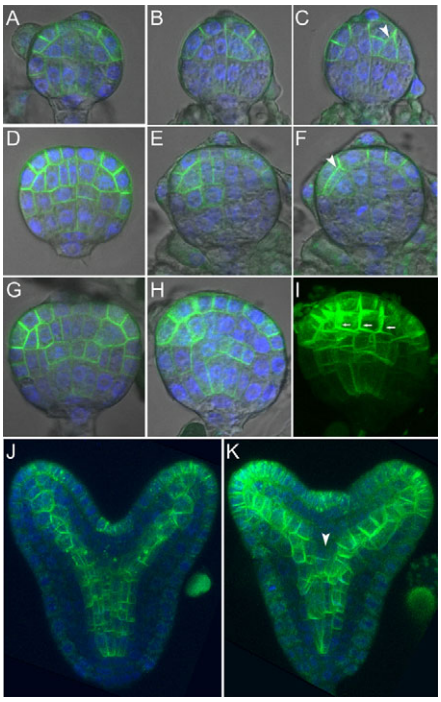

Fig. 4. Expression of PIN1:GFP in wild-type and *iaa18-1* embryos. (**A-C**) Wild-type (A) and *iaa18-1/IAA18* (B,C) early globular stage embryos. Arrowhead in (C) indicates misaligned periclinal cell division planes in adjacent L1 cells. (**D-F**) Wild-type (D) and *iaa18-1/IAA18* (E,F) mid-globular stage embryos. Arrowhead in F indicates an ectopic periclinal cell division. (**G-I**) Wild-type (G) and *iaa18-1/IAA18* (H,I) transition stage embryos. Small arrows in I indicate apparent polarity of PIN1:GFP localization away from the cotyledon primordium on the right. (**J**,**K**) Wild-type (J) and *iaa18-1/IAA18* (K) torpedo stage embryos. Arrowhead in K indicates a cell layer lacking fluorescence in the mutant embryo. (A-H) Optical sections (1 μm) through the central apical-basal axis of the embryo. (B,C,E,F) Adjacent sections through the same *iaa18-1/IAA18* early and mid-globular embryos, respectively. (I) A *z*-stack projection of the same *iaa18-1/IAA18* embryo as in H. (J,K) *Z*-stack projections of 16 1 μm sections through the central apical-basal axis of the embryo. Wild-type and mutant embryos were fixed, stained with DAPI and photographed in parallel using identical settings. (A-H) Overlays of fluorescent and DIC images. The *PIN1:GFP* lines used have been described previously (Heisler et al., 2005) (see Table S4 in the supplementary material).

et al., 2002; Bennett et al., 1995; Okada et al., 1991), it is likely that altered expression of *PIN1* (and possibly other *PIN* genes) in *iaa18-1* embryos contributes to subsequent cotyledon placement defects. Thus, some cotyledon anlagen cells may acquire insufficient auxin and fail to grow, whereas others may accumulate too much auxin and therefore overproliferate. Intercellular positive feedback might reinforce initial asymmetries in *PIN* expression; for example, to cause a single initiated cotyledon to occupy an enlarged domain that includes cells that normally form cotyledon margins. This model can explain why inhibiting auxin response symmetrically throughout the apical domain causes asymmetry in the resulting morphology. As auxin does not induce *IAA18* transcription, the *iaa18-1* mutant may be partially insulated from negative feedback that might normally promote robust patterning.

We observed *iaa18-1* globular embryos with asymmetric PIN1:GFP expression more frequently than seedlings with aberrant cotyledon placement, suggesting that many mutant embryos recover normal patterning, despite early PIN1 misexpression. Similarly, *pin1*, *pin7* and higher-order *pin* mutant seedlings often appear normal, despite having reduced embryonic *PIN* expression and exhibiting early cell division patterning defects (Blilou et al., 2005; Friml et al., 2003; Okada et al., 1991; Vieten et al., 2005). Although we could not follow individual embryos as they developed, a subset of embryos with asymmetric PIN1 expression, perhaps those with ectopic cell divisions or discontinuous vasculature, may later develop aberrant cotyledon outgrowth. Subsequently, at heart stage, absence of PIN1:GFP expression in sub-meristem cells and vascular discontinuities may arise from persistent action of IAA18-1, or as indirect consequences of earlier perturbed auxin transport.

Ectopic expression of *axr2/iaa7* or *slr/iaa14* gain-of-function mutant genes in transition and heart stage cotyledon primordia eliminated growth of one or both cotyledons, but did not affect cotyledon patterning as *iaa18-1* does (Muto et al., 2007). These results suggest that ARF function is necessary for cotyledon outgrowth, even after patterning has been established. It is therefore possible that, in addition to affecting *PIN* expression, IAA18-1 might affect expression of ARF target genes whose products drive cell expansion or cell division. IAA18-1 might decrease expression of such genes in cotyledon primordia and/or increase their expression in cotyledon margin zones. Although simple models of auxin response imply that gain-of-function *iaa* mutations should decrease ARF target gene expression, increases in expression might arise from decreased intracellular negative feedback or from decreased auxin efflux. Gain-of-function *axr3* mutants have increased auxin response in some assays, and also have accelerated hypocotyl growth as do *iaa18-1* seedlings (Leyser et al., 1996).

IAA18-1 affects activity of multiple ARF proteins

iaa18-1 and *mp* mutant embryos each have similar apical phenotypes, and the ability of overexpressed *MP/ARF5* to suppress *iaa18-1* phenotypes indicates that IAA18-1 can interact with MP/ARF5. MP/ARF5 is expressed and present throughout the embryo except in the L1 layer (Hamann et al., 2002; Hardtke and Berleth, 1998; Hardtke et al., 2004; Weijers et al., 2006), so IAA18-1 could inhibit MP/ARF5 in most apical domain cells.

As *iaa18-1* and *mp* mutations enhanced each other, IAA18-1 probably also targets other ARF proteins. ARF6, NPH4/ARF7, ARF8 and ARF19 are the most closely related ARF proteins to MP/ARF5 (Remington et al., 2004). *nph4* mutations enhanced *mp* mutations (Hardtke et al., 2004) but did not enhance *iaa18-1*, consistent with NPH4/ARF7 and IAA18-1 acting in a common pathway. Moreover, IAA18 can interact with NPH4/ARF7 and ARF19 in yeast two-hybrid assays, and the reduced frequency of lateral roots in *iaa18* plants also suggests that IAA18-1 may inhibit NPH4/ARF7 and ARF19 in roots (see Table S1 in the supplementary material) (Okushima et al., 2005; Uehara et al., 2008; Wilmoth et al., 2005). Similarly, *iaa18-1*, *arf6* and *arf8* mutants each have long hypocotyls and short stamen filaments (Nagpal et al., 2005; Tian et al., 2004), suggesting that IAA18-1 might inhibit ARF6 or ARF8. However, overexpression of *ARF6*, *NPH4/ARF7* or *ARF8* did not suppress *iaa18-1*. In addition. in a wild-type background, only *MP/ARF5* overexpression causes strong phenotypes (Hardtke et al., 2004; Wu et al., 2006). Regulation by the microRNA *miR167* apparently limits the effectiveness of *ARF6* and *ARF8* overexpression constructs (Wu et al., 2006). A higher degree of overexpression might be needed to accumulate enough ARF6, NPH4/ARF7 or ARF8 protein to suppress *iaa18-1* effects; for example, if translation of these ARF proteins is inefficient.

Alternatively, these ARF proteins may differ from MP/ARF5 in some functional attribute. Thus, in embryos, IAA18-1 may inhibit one or more of these ARF proteins, or other ARFs that we have not tested.

Similarly to *iaa18-1*, the *bdl* mutation decreased PIN1 expression, and inhibited MP/ARF5 function when driven by the *Q0990* GAL4-expressing line (Weijers et al., 2006). Moreover, *mp bdl* embryos lacked cotyledons, indicating that BDL/IAA12 also has targets in addition to MP/ARF5 (Hamann et al., 2002; Hamann et al., 1999). Together, IAA18-1 and BDL are expressed in all cells of globular and heart stage embryos, except the L1 layer on the abaxial flanks (Hamann et al., 2002; Weijers et al., 2006), so the presence of cotyledons in *iaa18-1/IAA18 bdl/BDL* embryos suggests either that the concentration of BDL or IAA18-1 was below a threshold required to inhibit the relevant ARF proteins fully, or that IAA18-1 and BDL proteins may attenuate the activity of each other, for example through protein-protein interactions. *IAA12/BDL* and *IAA18* may normally act partially redundantly. However, *bdl iaa18* double loss-of-function mutants developed normally. Higher-order loss-of-function mutants may reveal whether Aux/IAA proteins are in fact necessary for correct embryo patterning.

iaa18-1 affects axis and root pole development non-autonomously

Root formation depends on auxin response in the axis (Weijers et al., 2006), where *IAA18* is not expressed. Decreased root pole formation in *iaa18-1/ bdl/*, *iaa18-1/ axr1-13* and *iaa18-1/ tir1-1* double mutants, and the narrower domain of PIN1:GFP expression in the axis of *iaa18-1* heart and torpedo stage embryos, suggest that *iaa18-1* acts non-autonomously on axis cells. IAA18-1 might reduce apical to basal auxin flux, either by affecting auxin efflux from apical cells, or as an indirect consequence of altered apical patterning or cotyledon outgrowth. Consistent with these models, *WEI8/TAA1*, *YUCCA1* (*YUC1*), *YUC4*, *YUC10* and *YUC11* genes involved in tryptophan-dependent auxin biosynthesis are expressed in the apical domain of globular stage embryos, and embryonic root formation requires these *YUCCA* genes, as well as polar transport of auxin from apical to basal domains starting at the globular stage (Cheng et al., 2007; Friml et al., 2003; Steinmann et al., 1999; Stepanova et al., 2008).

We thank R. P. Elumalai for identifying the *iaa18-1* mutant, M. Ben-Davies for help with mapping, J. Dangl and S. Grant for use of their compound microscope, J. Haseloff for use of his confocal microscope, and L. Hobbie, E. Liscum, T. Berleth, J. Friml, M. Cha, M. Estelle, E. Meyerowitz and G. Jürgens for seeds of various genotypes. This work was funded by USDA grant 2001-02018 to P.N. and J.W.R., and by US National Institutes of Health grant GM52456 to J.W.R. Deposited in PMC for release after 12 months.

Supplementary material

Supplementary material for this article is available at http://dev.biologists.org/cgi/content/full/136/9/1509/DC1

References

Aida, M., Vernoux, T., Furutani, M., Traas, J. and Tasaka, M. (2002). Roles of *PIN-FORMED1* and *MONOPTEROS* in pattern formation of the apical region of the *Arabidopsis* embryo. *Development* **129**, 3965-3974.

Benjamins, R., Quint, A., Weijers, D., Hooykaas, P. and Offringa, R. (2001). The PINOID protein kinase regulates organ development in Arabidopsis by enhancing polar auxin transport. *Development* **128**, 4057-4067.

Benkova, E., Michniewicz, M., Sauer, M., Teichmann, T., Seifertova, D., Jurgens, G. and Friml, J. (2003). Local, efflux-dependent auxin gradients as a common module for plant organ formation. *Cell* **115**, 591-602.

Bennett, S. R. M., Alvarez, J., Bossinger, G. and Smyth, D. R. (1995). Morphogenesis in pinoid mutants of *Arabidopsis thaliana*. *Plant J.* **8**, 505-520.

Berleth, T. and Jürgens, G. (1993). The role of the *monopteros* gene in organising the basal body region of the *Arabidopsis* embryo. *Development* **118**, 575-587.

Blilou, I., Xu, J., Wildwater, M., Willemsen, V., Paponov, I., Friml, J., Heidstra, R., Aida, M., Palme, K. and Scheres, B. (2005). The PIN auxin efflux facilitator network controls growth and patterning in Arabidopsis roots. *Nature* **433**, 39-44.

Cheng, Y., Dai, X. and Zhao, Y. (2007). Auxin synthesized by the YUCCA flavin monooxygenases is essential for embryogenesis and leaf formation in Arabidopsis. *Plant Cell* **19**, 2430-2439.

Dharmasiri, N., Dharmasiri, S., Jones, A. M. and Estelle, M. (2003). Auxin action in a cell-free system. *Curr. Biol.* **13**, 1418-1422.

Dharmasiri, N., Dharmasiri, S. and Estelle, M. (2005a). The F-box protein TIR1 is an auxin receptor. *Nature* **435**, 441-445.

Dharmasiri, N., Dharmasiri, S., Weijers, D., Lechner, E., Yamada, M., Hobbie, L., Ehrismann, J. S., Jürgens, G. and Estelle, M. (2005b). Plant development is regulated by a family of Auxin Receptor F Box proteins. *Dev. Cell* **9**, 109-119.

Dharmasiri, N., Dharmasiri, S., Weijers, D., Karunarathna, N., Jurgens, G. and Estelle, M. (2007). AXL and AXR1 have redundant functions in RUB conjugation and growth and development in Arabidopsis. *Plant J.* **52**, 114-123.

Friml, J., Benkova, E., Blilou, I., Wisniewska, J., Hamann, T., Ljung, K., Woody, S., Sandberg, G., Scheres, B., Jurgens, G. et al. (2002). AtPIN4 mediates sink-driven auxin gradients and root patterning in Arabidopsis. *Cell* **108**, 661-673.

Friml, J., Vieten, A., Sauer, M., Weijers, D., Schwarz, H., Hamann, T., Offringa, R. and Jurgens, G. (2003). Efflux-dependent auxin gradients establish the apical-basal axis of Arabidopsis. *Nature* **426**, 147-153.

Friml, J., Yang, X., Michniewicz, M., Weijers, D., Quint, A., Tietz, O., Benjamins, R., Ouwerkerk, P. B., Ljung, K., Sandberg, G. et al. (2004). A PINOID-dependent binary switch in apical-basal PIN polar targeting directs auxin efflux. *Science* **306**, 862-865.

Furutani, M., Vernoux, T., Traas, J., Kato, T., Tasaka, M. and Aida, M. (2004). PIN-FORMED1 and PINOID regulate boundary formation and cotyledon development in Arabidopsis embryogenesis. *Development* **131**, 5021-5030.

Galweiler, L., Guan, C., Muller, A., Wisman, E., Mendgen, K., Yephremov, A. and Palme, K. (1998). Regulation of polar auxin transport by AtPIN1 in Arabidopsis vascular tissue. *Science* **282**, 2226-2230.

Gray, W., Kepinski, S., Rouse, D., Leyser, O. and Estelle, M. (2001). Auxin regulates SCF^{TIR1}-dependent degradation of AUX/IAA proteins. *Nature* **414**, 271-276.

Guilfoyle, T. J. and Hagen, G. (2007). Auxin response factors. *Curr. Opin. Plant Biol.* **10**, 453-460.

Hajdukiewicz, P., Svab, Z. and Maliga, P. (1994). The small, versatile *pPZP* family of *Agrobacterium* binary vectors for plant transformation. *Plant Mol. Biol.* **25**, 989-994.

Hamann, T., Mayer, U. and Jürgens, G. (1999). The auxin-insensitive *bodenlos* mutation affects primary root formation and apical-basal patterning in the *Arabidopsis* embryo. *Development* **126**, 1387-1395.

Hamann, T., Benkova, E., Baurle, I., Kientz, M. and Jurgens, G. (2002). The *Arabidopsis BODENLOS* gene encodes an auxin response protein inhibiting MONOPTEROS-mediated embryo patterning. *Genes Dev.* **16**, 1610-1615.

Hardtke, C. S. and Berleth, T. (1998). The *Arabidopsis* gene *MONOPTEROS* encodes a transcription factor mediating embryo axis formation and vascular development. *EMBO J.* **17**, 1405-1411.

Hardtke, C. S., Ckurshumova, W., Vidaurre, D. P., Singh, S. A., Stamatiou, G., Tiwari, S. B., Hagen, G., Guilfoyle, T. J. and Berleth, T. (2004). Overlapping and non-redundant functions of the Arabidopsis auxin response factors MONOPTEROS and NONPHOTOTROPIC HYPOCOTYL 4. *Development* **131**, 1089-1100.

Haseloff, J., Dormand, E. L. and Brand, A. H. (1999). Live imaging with green fluorescent protein. *Methods Mol. Biol.* **122**, 241-259.

Heisler, M. G., Ohno, C., Das, P., Sieber, P., Reddy, G. V., Long, J. A. and Meyerowitz, E. M. (2005). Patterns of auxin transport and gene expression during primordium development revealed by live imaging of the arabidopsis inflorescence meristem. *Curr. Biol.* **15**, 1899-1911.

Hobbie, L., McGovern, M., Hurwitz, L. R., Pierro, A., Liu, N. Y., Bandyopadhyay, A. and Estelle, M. (2000). The *axr6* mutants of *Arabidopsis thaliana* define a gene involved in auxin response and early development. *Development* **127**, 23-32.

Karimi, M., Inze, D. and Depicker, A. (2002). GATEWAY™ vectors for *Agrobacterium*-mediated plant transformation. *Trends Plant Sci.* **17**, 193-195.

Kepinski, S. and Leyser, O. (2004). Auxin-induced SCFTIR1-Aux/IAA interaction involves stable modification of the SCFTIR1 complex. *Proc. Natl. Acad. Sci. USA* **101**, 12381-12386.

Kepinski, S. and Leyser, O. (2005). The Arabidopsis F-box protein TIR1 is an auxin receptor. *Nature* **435**, 446-451.

Leyser, H. M. O., Pickett, F. B., Dharmasiri, S. and Estelle, M. (1996). Mutations in the *AXR3* gene of *Arabidopsis* result in altered auxin response including ectopic expression from the *SAUR-AC1* promoter. *Plant J.* **10**, 403-413.

Liscum, E. and Briggs, W. R. (1996). Mutations of Arabidopsis in potential transduction and response components of the phototropic signaling pathway. *Plant Physiol.* **112**, 291-296.

Long, J. A. and Barton, M. K. (1998). The development of apical embryonic pattern in *Arabidopsis*. *Development* **125**, 3027-3035.
Mallory, A. C., Bartel, D. P. and Bartel, B. (2005). MicroRNA-directed regulation of arabidopsis AUXIN RESPONSE FACTOR17 is essential for proper development and modulates expression of early auxin response genes. *Plant Cell* **17**, 1360-1375.
Muto, H., Watahiki, M. K., Nakamoto, D., Kinjo, M. and Yamamoto, K. T. (2007). Specificity and similarity of functions of the Aux/IAA genes in auxin signaling of Arabidopsis revealed by promoter-exchange experiments among MSG2/IAA19, AXR2/IAA7, and SLR/IAA14. *Plant Physiol.* **144**, 187-196.
Nagpal, P., Ellis, C. M., Weber, H., Ploense, S. E., Barkawi, L. S., Guilfoyle, T. J., Hagen, G., Alonso, J. M., Cohen, J. D., Farmer, E. E. et al. (2005). Auxin Response Factors ARF6 and ARF8 promote jasmonic acid production and flower maturation. *Development* **132**, 4107-4118.
Okada, K., Ueda, J., Komaki, M. K., Bell, C. J. and Shimura, Y. (1991). Requirement of the auxin polar transport system in early stages of *Arabidopsis* floral bud formation. *Plant Cell* **3**, 677-684.
Okushima, Y., Overvoorde, P. J., Arima, K., Alonso, J. M., Chan, A., Chang, C., Ecker, J. R., Hughes, B., Lui, A., Nguyen, D. et al. (2005). Functional genomic analysis of the AUXIN RESPONSE FACTOR gene family members in arabidopsis thaliana: unique and overlapping functions of ARF7 and ARF19. *Plant Cell* **17**, 444-463.
Paciorek, T., Zazimalova, E., Ruthardt, N., Petrasek, J., Stierhof, Y. D., Kleine-Vehn, J., Morris, D. A., Emans, N., Jurgens, G., Geldner, N. et al. (2005). Auxin inhibits endocytosis and promotes its own efflux from cells. *Nature* **435**, 1251-1256.
Przemeck, G. K. H., Mattsson, J., Hardtke, C. S., Sung, Z. R. and Berleth, T. (1996). Studies on the role of the *Arabidopsis* gene *MONOPTEROS* in vascular development and plant cell axialization. *Planta* **200**, 229-237.
Ramos, J., Zenser, N., Leyser, O. and Callis, J. (2001). Rapid degradation of auxin/indoleacetic acid proteins requires conserved amino acids of domain II and is proteasome dependent. *Plant Cell* **13**, 2349-2360.
Reed, J. W. (2001). Roles and Activitiesof Aux/IAA proteins in *Arabidopsis*. *Trends Plant Sci.* **6**, 420-425.
Reinhardt, D., Mandel, T. and Kuhlemeier, C. (2000). Auxin regulates the initiation and radial position of plant lateral organs. *Plant Cell* **12**, 507-518.
Reinhardt, D., Pesce, E. R., Stieger, P., Mandel, T., Baltensperger, K., Bennett, M., Traas, J., Friml, J. and Kuhlemeier, C. (2003). Regulation of phyllotaxis by polar auxin transport. *Nature* **426**, 255-260.
Remington, D. L., Vision, T. J., Guilfoyle, T. J. and Reed, J. W. (2004). Contrasting modes of diversification in the Aux/IAA and ARF gene families. *Plant Physiol.* **135**, 1738-1752.
Sabatini, S., Beis, D., Wolkenfelt, H., Murfett, J., Guilfoyle, T., Malamy, J., Benfey, P., Leyser, O., Bechtold, N., Weisbeek, P. et al. (1999). An auxin-dependent distal organizer of pattern and polarity in the *Arabidopsis* root. *Cell* **99**, 463-472.
Sauer, M., Balla, J., Luschnig, C., Wisniewska, J., Reinohl, V., Friml, J. and Benkova, E. (2006a). Canalization of auxin flow by Aux/IAA-ARF-dependent feedback regulation of PIN polarity. *Genes Dev.* **20**, 2902-2911.
Sauer, M., Paciorek, T., Benkova, E. and Friml, J. (2006b). Immunocytochemical techniques for whole-mount in situ protein localization in plants. *Nat. Protoc.* **1**, 98-103.
Schuetz, M., Berleth, T. and Mattsson, J. (2008). Multiple MONOPTEROS-dependent pathways are involved in leaf initiation. *Plant Physiol.* **148**, 870-880.
Steinmann, T., Geldner, N., Grebe, M., Mangold, S., Jackson, C. L., Paris, S., Gälweiler, L., Palme, K. and Jürgens, G. (1999). Coordinated polar localization of auxin efflux carrier PIN1 by GNOM ARF GEF. *Science* **286**, 316-318.
Stepanova, A. N., Robertson-Hoyt, J., Yun, J., Benavente, L. M., Xie, D. Y., Dolezal, K., Schlereth, A., Jurgens, G. and Alonso, J. M. (2008). TAA1-mediated auxin biosynthesis is essential for hormone crosstalk and plant development. *Cell* **133**, 177-191.
Szemenyei, H., Hannon, M. and Long, J. A. (2008). TOPLESS mediates auxin-dependent transcriptional repression during Arabidopsis embryogenesis. *Science* **319**, 1384-1386.
Tan, X., Calderon-Villalobos, L. I., Sharon, M., Zheng, C., Robinson, C. V., Estelle, M. and Zheng, N. (2007). Mechanism of auxin perception by the TIR1 ubiquitin ligase. *Nature* **446**, 640-645.
Tatematsu, K., Kumagai, S., Muto, H., Sato, A., Watahiki, M. K., Harper, R. M., Liscum, E. and Yamamoto, K. T. (2004). MASSUGU2 encodes Aux/IAA19, an auxin-regulated protein that functions together with the transcriptional activator NPH4/ARF7 to regulate differential growth responses of hypocotyl and formation of lateral roots in Arabidopsis thaliana. *Plant Cell* **16**, 379-393.
Tian, C., Muto, H., Higuchi, K., Matamura, T., Tatematsu, K., Koshiba, T. and Yamamoto, K. T. (2004). Disruption and overexpression of *auxin response factor 8* gene of Arabidopsis affect hypocotyl elongation and root growth habit, indicating its possible involvement in auxin homeostasis in light condition. *Plant J.* **40**, 333-343.
Tian, Q. and Reed, J. (1999). Control of auxin-regulated root development by the Arabidopsis thaliana *SHY2/IAA3* gene. *Development* **126**, 711-721.
Tian, Q., Uhlir, N. J. and Reed, J. W. (2002). Arabidopsis SHY2/IAA3 inhibits auxin-regulated gene expression. *Plant Cell* **14**, 301-319.
Tian, Q., Nagpal, P. and Reed, J. W. (2003). Regulation of *Arabidopsis* SHY2/IAA3 protein turnover. *Plant J.* **36**, 643-651.
Tiwari, S. B., Hagen, G. and Guilfoyle, T. J. (2004). Aux/IAA proteins contain a potent transcriptional repression domain. *Plant Cell* **16**, 533-543.
Tiwari, S. B., Wang, X. J., Hagen, G. and Guilfoyle, T. J. (2001). AUX/IAA proteins are active repressors, and their stability and activity are modulated by auxin. *Plant Cell* **13**, 2809-2822.
Truernit, E., Siemering, K. R., Hodge, S., Grbic, V. and Haseloff, J. (2006). A map of KNAT gene expression in the Arabidopsis root. *Plant Mol. Biol.* **60**, 1-20.
Uehara, T., Okushima, Y., Mimura, T., Tasaka, M. and Fukaki, H. (2008). Domain II mutations in CRANE/IAA18 suppress lateral root formation and affect shoot development in *Arabidopsis thaliana*. *Plant Cell Physiol.* **49**, 1025-1038.
Ulmasov, T., Hagen, G. and Guilfoyle, T. J. (1997a). ARF1, a transcription factor that binds to auxin response elements. *Science* **276**, 1865-1868.
Ulmasov, T., Murfett, J., Hagen, G. and Guilfoyle, T. J. (1997b). Aux/IAA proteins repress expression of reporter genes containing natural and highly active synthetic auxin response elements. *Plant Cell* **9**, 1963-1971.
Ulmasov, T., Hagen, G. and Guilfoyle, T. J. (1999a). Activation and repression of transcription by auxin-response factors. *Proc. Natl. Acad. Sci. USA* **96**, 5844-5849.
Ulmasov, T., Hagen, G. and Guilfoyle, T. J. (1999b). Dimerization and DNA binding of auxin response factors. *Plant J.* **19**, 309-319.
Vernoux, T., Kronenberger, J., Grandjean, O., Laufs, P. and Traas, J. (2000). *PIN-FORMED 1* regulates cell fate at the periphery of the shoot apical meristem. *Development* **127**, 5157-5165.
Vieten, A., Vanneste, S., Wisniewska, J., Benkova, E., Benjamins, R., Beeckman, T., Luschnig, C. and Friml, J. (2005). Functional redundancy of PIN proteins is accompanied by auxin-dependent cross-regulation of PIN expression. *Development* **132**, 4521-4531.
Walsh, T. A., Neal, R., Merlo, A. O., Honma, M., Hicks, G. R., Wolff, K., Matsumura, W. and Davies, J. P. (2006). Mutations in an auxin receptor homolog AFB5 and in SGT1b confer resistance to synthetic picolinate auxins and not to 2,4-dichlorophenoxyacetic acid or indole-3-acetic acid in Arabidopsis. *Plant Physiol.* **142**, 542-552.
Weijers, D., Benkova, E., Jäger, K. E., Schlereth, A., Hamann, T., Kientz, M., Wilmoth, J. C., Reed, J. W. and Jürgens, G. (2005a). Developmental specificity of auxin response by pairs of ARF and Aux/IAA transcriptional regulators. *EMBO J.* **24**, 1874-1885.
Weijers, D., Sauer, M., Meurette, O., Friml, J., Ljung, K., Sandberg, G., Hooykaas, P. and Offringa, R. (2005b). Maintenance of embryonic Auxin distribution for apical-basal patterning by PIN-FORMED-dependent auxin transport in *Arabidopsis*. *Plant Cell* **17**, 2517-2526.
Weijers, D., Schlereth, A., Ehrismann, J. S., Schwank, G., Kientz, M. and Jurgens, G. (2006). Auxin triggers transient local signaling for cell specification in Arabidopsis embryogenesis. *Dev. Cell* **10**, 265-270.
Wenzel, C. L., Schuetz, M., Yu, Q. and Mattsson, J. (2007). Dynamics of MONOPTEROS and PIN-FORMED1 expression during leaf vein pattern formation in Arabidopsis thaliana. *Plant J.* **49**, 387-398.
Wilmoth, J. C., Wang, S., Tiwari, S. B., Joshi, A. D., Hagen, G., Guilfoyle, T. J., Alonso, J. M., Ecker, J. R. and Reed, J. W. (2005). NPH4/ARF7 and ARF19 promote leaf expansion and auxin-induced lateral root formation. *Plant J.* **43**, 118-130.
Wu, M.-F., Tian, Q. and Reed, J. W. (2006). *Arabidopsis microRNA167* controls patterns of *ARF6* and *ARF8* expression and regulates both female and male reproduction. *Development* **133**, 4211-4218.
Yang, X., Lee, S., So, J.-h., Dharmasiri, S., Dharmasiri, N., Ge, L., Jensen, C., Hangarter, R., Hobbie, L. and Estelle, M. (2004). The IAA1 protein is encoded by *AXR5* and is a substrate of SCF^{TIR1}. *Plant J.* **40**, 772-782.
Zenser, N., Ellsmore, A., Leasure, C. and Callis, J. (2001). Auxin modulates the degradation rate of Aux/IAA proteins. *Proc. Natl. Acad. Sci. USA* **98**, 11795-11800.

Table S1. Seedling growth phenotypes*

	L*er*	IAA18-1/iaa18-1	iaa18-1/iaa18-1
Hypocotyl length in light (mm)†	2.8 (0.4)	nd	5.7 (0.5)
Hypocotyl length in dark (mm)†	18.5 (2.0)	nd	16.0 (1.3)
Lateral root number‡	48.2 (6.6)	39.2 (8.3)	1.6 (1.4)
Root length (mm)§	26.1 (6.3)	11.8 (3.4)	7.9 (3.0)

*Data are means (s.d.).

†Seedlings were grown on 1× MS plates in constant light or darkness for 6 days (*n*=40).

‡Seedlings were grown on 1× MS, 1% sucrose plates for 20 days under long day conditions (*n*=20).

§Seedlings were grown on 1× MS, 1% sucrose plates for 7 days under constant light (*n*=25).

Table S2. Numbers of floral organs

	Sepals	Petals	Stamens	Carpels
Wild type (L*er*)	4.02 (0.16)	4.02 (0.16)	5.5 (0.71)	2 (0)
iaa18-1/IAA18-1	4 (0)	3.93 (0.35)	5.33 (0.72)	2 (0)
iaa18-1/iaa18-1	3.93 (0.35)	3.35 (0.88)*	4.45 (0.59)*	2 (0)
bdl/BDL	4 (0)	3.95 (0.22)	5.2 (0.72)	2 (0)
iaa18-1/IAA18 bdl/BDL	3.93 (0.26)	2.25 (0.89)*	4.53 (0.74)*	1.98 (0.16)

Plants were grown in long days. Data are means (s.d.) from 40 flowers.
*Significant difference from the mean wild-type value by *t*-test ($P<0.05$).

Table S3. Recapitulation of *iaa18-1* phenotypes in T1 seedlings

Transgene	Number screened	Number in each phenotypic class (Number surviving to adulthood)			
		No root	Aberrant phyllotaxy	Unopened cotyledons	Curled leaves
iaa18-1:GUS	15,000	34 (0)	41 (2)	14 (4)	3 (3)
iaa18-1	4,000	3 (0)	8 (0)	0	nd

T1 seedlings selected for hygromycin resistance carrying either the *iaa18-1* or *iaa18-1:GUS* genomic constructs either failed to survive, or they had no morphological phenotype or GUS activity suggesting that the transgene had been silenced. We therefore screened without antibiotic selection among T1 seedlings for those with aberrant cotyledon placement. T1 seeds from L*er* plants infiltrated with *iaa18-1:GUS* or from Columbia plants infiltrated with *iaa18-1* were plated without selection, and the number of seedlings with each phenotype counted. Seedlings in the 'no root' category generally also had aberrant phyllotaxy. Fig. S2 shows *iaa18-1:GUS* seedlings representative of different phenotypic classes. For representative *iaa18-1:GUS* transformants, we confirmed by subsequent X-Gluc staining that seedlings with phenotypes indeed carried the *iaa18-1:GUS* transgene. Numbers in parentheses indicate the number of seedlings in each category that survived to adulthood. Phenotypes of these surviving transformants often disappeared late in development and in subsequent generations. nd, not determined.

Table S4. Frequency of asymmetric PIN1:GFP expression in wild-type and *iaa18-1/IAA18* embryos*

	Early globular stage		Mid-globular stage		Late globular/transition stage	
Embryo genotype	*IAA18/IAA18*	*iaa18-1/IAA18*	*IAA18/IAA18*	*iaa18-1/IAA18*	*IAA18/IAA18*	*iaa18-1/IAA18*
Experiment 1†	1/22 (5%)	5/13 (38%)	0/23 (0%)	6/11 (55%)	0/5 (0%)	1/3 (33%)
Experiment 2†	0/12 (0%)	5/38 (13%)	0/19 (0%)	8/23 (35%)	0/11 (0%)	1/4 (25%)
Experiment 3†	0/27 (0%)	3/17 (18%)†	0/26 (0%)	7/18 (39%)†	0/17 (0%)	2/4 (50%)†
Total	1/61 (2%)	13/68 (19%)	0/68 (0%)	21/52 (40%)	0/33 (0%)	4/11 (36%)

*Shown are numbers of embryos with asymmetric PIN1:GFP expression over number of embryos observed, and calculated percentages (in parentheses).

†In experiments 1 and 2, pollen from wild-type or *iaa18-1* homozygous plants was used to pollinate homozygous marker lines that were wild-type at *IAA18*. In experiment 3, a plant homozygous for P_{PIN1}*:PIN1:GFP* and heterozygous for *iaa18-1* was selfed, and '*iaa18-1/+*' embryos were therefore actually a mixture of wild-type, *iaa18-1/IAA18* and *iaa18-1/iaa18-1* genotypes in roughly 1:2:1 ratio. In experiment 1, we used a P_{PIN1}*:PIN1:GFP* P_{REV}*:REV:Venus* P_{FIL}*:DsRED* marker line, and in experiments 2 and 3 we used a P_{PIN1}*:PIN1:GFP* P_{STM}*:YFP* P_{WUS}*:DsRED* line. Expression of P_{REV}*:REV:Venus*, P_{FIL}*:DsRED*, P_{STM}*:YFP* and P_{WUS}*:DsRED* markers in these lines were not analyzed.

Table S5. Rescue of *IAA* gain-of-function phenotypes by *ARF* overexpression

T1 plant genotype	Number of transformants	Number with flat leaves (terminal pin or flower)
P_{35S}:MP/ARF5	103	103 (13)
iaa18-1/ P_{35S}:MP/ARF5	79	28 (0)
bdl/ P_{35S}:MP/ARF5	58	16 (0)
P_{35S}:NPH4/ARF7	10	10
iaa18-1/ P_{35S}:NPH4 /ARF7	6	0
bdl/ P_{35S}:NPH4/ARF7	8	0
P_{35S}:ARF6	33	33
iaa18-1/ P_{35S}:ARF6	54	0
bdl/ P_{35S}:ARF6	23	0
P_{35S}:ARF8	93	93
iaa18-1/ P_{35S}:ARF8	123	0
bdl/ P_{35S}:ARF8	48	0

Numbers of transformants in wild-type backgrounds are pooled results from transformations into *iaa18-1/IAA18* or *bdl/BDL* parent plants. Plants with flat leaves were genotyped for *iaa18-1* or *bdl* mutations using PCR-based assays. Two of the *iaa18-1/ P_{35S}:MP/ARF5* plants were homozygous for *iaa18-1*. Numbers of *P_{35S}:MP/ARF5* transformants with a terminal pin or flower structure on the inflorescence are indicated in parentheses. In addition to T1 transformants listed, we also crossed a *P_{35S}:NPH4/ARF7* line with *iaa18-1/IAA18*, and failed to see suppression of *iaa18-1* vegetative phenotypes among *iaa18-1/IAA18 P_{35S}:NPH4/ARF7/-* F1 plants.